







DSOK-0011 Potentially Regulates Circadian Misalignment and Affects Gut Microbiota Composition in Activity-Based Anorexia Model

¹Department of Neuropsychiatry, Okayama University Graduate School of Medicine, Dentistry and Pharmaceutical Sciences, Okayama, Japan | ²Okayama University Medical School, Okayama, Japan | ³Department of Neuropsychiatry, Okayama University Hospital, Okayama, Japan | ⁴Sumitomo Pharma Co. Ltd, Osaka, Japan | ⁵Department of Animal Applied Microbiology, Okayama University Graduate School of Environmental, Life, Natural Science and Technology, Okayama, Japan | ⁶Department of Molecular Biology and Biochemistry, Okayama University Graduate School of Medicine, Dentistry and Pharmaceutical Sciences, Okayama, Japan | ⁷Department of Molecular Biology and Biochemistry, Okayama University Faculty of Medicine, Dentistry and Pharmaceutical Sciences, Okayama, Japan | ⁸Department of Neuropsychiatry, Okayama University Faculty of Medicine, Dentistry and Pharmaceutical Sciences, Okayama, Japan | ⁸Department of Neuropsychiatry, Okayama University Faculty of Medicine, Dentistry and Pharmaceutical Sciences, Okayama, Japan | ⁸Department of Neuropsychiatry, Okayama University Faculty of Medicine, Dentistry and Pharmaceutical Sciences, Okayama, Japan | ⁸Department of Neuropsychiatry, Okayama University Faculty of Medicine, Dentistry and Pharmaceutical Sciences, Okayama, Japan | ⁸Department of Neuropsychiatry, Okayama University Faculty of Medicine, Dentistry and Pharmaceutical Sciences, Okayama, Japan | ⁸Department of Neuropsychiatry, Okayama University Faculty of Medicine, Dentistry and Pharmaceutical Sciences, Okayama, Japan | ⁸Department of Neuropsychiatry, Okayama University Faculty of Medicine, Dentistry and Pharmaceutical Sciences, Okayama, Japan | ⁸Department of Neuropsychiatry, Okayama University Faculty of Medicine, Dentistry and Pharmaceutical Sciences, Okayama, Japan | ⁸Department of Neuropsychiatry, Okayama University Faculty of Medicine, Dentistry and Pharmaceutical Sciences, Okayama, Japan | ⁸Department of Neuropsychiatry, Okayama University Faculty of Medicine, Dentistry and Pharmaceutic

Correspondence: Shinji Sakamoto (ssakamoto@okayama-u.ac.jp)

Received: 28 April 2025 | Revised: 4 September 2025 | Accepted: 15 September 2025

Action Editor: Scott J. Crow

Funding: This work was supported by the Oofuji Endocrine Medical Award 2023, Japan Society for the Promotion of Science (22K07616, 23H04235, 24K10679, 24K10733, 24KK0155, and 25K19080), and Sumitomo Pharma Co. Ltd.

Keywords: 11β-HSD1 | activity-based anorexia | anorexia nervosa | corticosterone | eating disorders | microbiota

ABSTRACT

Objective: Anorexia nervosa (AN) is a metabolic-psychiatric disorder characterized by severe weight loss, hypercortisolemia, and hypothalamic-pituitary-adrenal (HPA) axis activation. In this study, we investigated the effect of inhibiting cortisol regeneration via the enzyme 11β -hydroxysteroid dehydrogenase type 1 (11β -HSD1) on the pathophysiology of AN.

Method: Female C57BL/6J mice underwent a 7-day activity-based anorexia (ABA) paradigm, involving 3h daily feeding and free access to wheels, until 25% body weight loss or experiment completion. Mice were orally treated once daily with a potent 11β -HSD1 inhibitor, DSOK-0011, or vehicle. Body weight, food intake, and activity transitions were recorded; plasma corticosterone and cholesterol levels were measured using a fluorometric assay; gut microbiota were analyzed using 16S rRNA sequencing; and hippocampal glial cells were analyzed using immunohistochemistry.

Results: DSOK-0011-treated mice exhibited a modest but significant increase in postprandial wheel-running activity compared to baseline (4–5 p.m., p = 0.018; 5–6 p.m., p = 0.043), whereas vehicle-treated mice showed higher preprandial activity (9–10 a.m., p = 0.0229). Gut microbiota analysis revealed increased alpha diversity in ABA mice, with a specific enrichment of the *Lachnospiraceae* family in the DSOK-0011 group. However, DSOK-0011 did not significantly affect body weight, food intake, corticosterone, and lipid levels, or hippocampal glial cell populations.

Hiroki Kawai and Nanami Wada contributed equally to this study.

This is an open access article under the terms of the Creative Commons Attribution-NonCommercial License, which permits use, distribution and reproduction in any medium, provided the original work is properly cited and is not used for commercial purposes.

© 2025 The Author(s). International Journal of Eating Disorders published by Wiley Periodicals LLC.

Conclusion: Inhibition of 11β -HSD1 by DSOK-0011 was associated with microbiota alterations and subtle shifts in activity timing under energy-deficient conditions. These findings suggest that peripheral glucocorticoid metabolism may influence microbial and behavioral responses in the ABA model, although its metabolic impact appears limited in the acute phase.

1 | Introduction

Anorexia nervosa (AN) is a metabo-psychiatric disorder characterized by an intense fear of weight gain and voluntary food restriction (FR), leading to life-threatening weight loss (Watson et al. 2019; Schalla and Stengel 2019). Most patients with AN exhibit excessive exercise, which hinders weight recovery by increasing energy expenditure (Zipfel et al. 2013). Due to severe underweight and poor treatment response, AN has one of the highest mortality rates among mental illnesses (Treasure et al. 2020; Iwajomo et al. 2021). Currently, there are no established psychopharmacological treatments to effectively manage the clinical course of AN.

Notably, the hypothalamic-pituitary-adrenal (HPA) axis plays a central role in both stress response and energy homeostasis (Zhang and Dulawa 2021; Haines 2023). Starvation and physical activity, the major characteristics of AN, are known to activate the HPA axis and induce hypersecretion of corticotropin-releasing hormone (CRH) (Fediuc et al. 2006; Droste et al. 2007), which in turn triggers the release of adrenalderived glucocorticoids (GC), primarily cortisol in humans and corticosterone in rodents (Joseph and Whirledge 2017). Previous studies have reported the anorexigenic effect of CRH, and its central injection has been shown to increase physical activity (Lawson et al. 2013; Krahn et al. 1988). Moreover, central CRH antagonism has been demonstrated to reverse appetite and weight loss in animals (Menzaghi et al. 1994; Spina et al. 2000; Kawaguchi et al. 2005; Mogami et al. 2016). Furthermore, hypercortisolemia, a typical indicator of HPA axis dysregulation, can alter the neuroendocrine signaling pathways involved in energy balance and feeding behavior (Balsevich et al. 2019). Clinical findings suggest that hypercortisolemia can be a predictor of treatment resistance in patients with AN and mood disorders (Fischer et al. 2017; Het et al. 2020; Markopoulou et al. 2021). CRH and cortisol hypersecretion are often considered as a compensatory mechanism and a physiological adaptive response to chronic malnutrition (Amorim et al. 2023). While cortisol levels normalize following weight restoration in many cases, several findings indicate that HPA axis dysregulation, including cortisol responsiveness to stress stimuli, persists even after weight recovery and may be involved in the pathophysiology of the disease itself (Herpertz-Dahlmann and Remschmidt 1990; Schmalbach et al. 2020; Kinzig and Hargrave 2010; Lee and Kinzig 2017).

 11β -hydroxysteroid dehydrogenase type 1 (11β -HSD1) is a key metabolic enzyme that amplifies intracellular GC activation by generating cortisol from its biologically inactive precursor cortisone (11-dehydrocorticosterone in rodents) (Gathercole et al. 2013). This enzyme contributes to tissue-specific cortisol production in the periphery (Stomby et al. 2014; Podraza et al. 2024), functions as an exclusive activator of GC in the central nervous system (Rajan et al. 1996), and acts as a regulator of basal activity of the HPA axis (Sandeep et al. 2004; Bisschop

et al. 2013). In metabolic stress conditions, 11β -HSD1 also influences cholesterol metabolism through increased local GC generation (Chapman et al. 2013). Notably, 11β -HSD1 is highly expressed in the hippocampus and modulates local levels of corticosterone, which in turn affects integrative approach aimed (Yau, Noble, et al. 2015). In addition, 11β-HSD1 activity has been shown to affect gut microbiota composition in a diet-dependent manner, highlighting its involvement in both brain function and gut homeostasis (Johnson et al. 2016). Considering that gut dysbiosis is strongly implicated in AN pathophysiology (Fan et al. 2023), interactions between microbiota and neuroendocrine regulation via 11β-HSD1 may represent a key mechanistic link. Gut bacteria are capable of modulating host neuroendocrine systems through microbial metabolites, immune signaling, and vagal pathways, thereby influencing stress responsiveness and feeding behavior (van de Wouw et al. 2017; Wiklund et al. 2021). AN patients often exhibit adaptive hypercholesterolemia, particularly during refeeding, which associates with increasing the risk of cardiovascular complications (García-Rubira et al. 1994; Abuzeid and Glover 2011). Given that 11β -HSD1 is implicated in both GC metabolism and cholesterol regulation, it emerges as a potential therapeutic target in addressing the metabolic and neuroendocrine dysregulation of AN.

Although the therapeutic effects of 11β -HSD1 inhibitor have been widely studied in metabolic disorders such as obesity and Type II diabetes mellitus (Anagnostis et al. 2013; Hu et al. 2013; Park et al. 2014; Othonos et al. 2023), their potential application in eating disorders remains largely unexplored. Despite the abundance of evidence implicating GC as a significant contributor to psychiatric symptoms, studies on the potential therapeutic benefits of 11β -HSD1 inhibitors are limited to dementia (Dodd et al. 2022). Importantly, several studies have shown that 11β -HSD1 inhibition may act as a potential HPA axis stabilizer without triggering compensatory activation (Berthiaume et al. 2007; Courtney et al. 2008; Hermanowski-Vosatka et al. 2005). However, no studies to date have assessed the effects of 11β -HSD1 inhibition in the context of AN.

To address this gap, we investigated the therapeutic potential of a novel 11β -HSD1 inhibitor, DSOK-0011 (described in WO-2011059021 as a potent inhibitor of 11β -HSD1 (Horiuchi et al. 2011)), in the activity-based anorexia (ABA) mouse model, which recapitulates key features of AN, including HPA axis dysregulation and excessive physical activity (Zhang and Dulawa 2021). We evaluated its impact on body weight, appetite, physical activity, and circulating corticosterone and cholesterol levels. Furthermore, to elucidate the mechanisms linking GC metabolism, gut function, and neuroinflammation, we examined changes in gut microbiota composition and hippocampal glial cells—both microglia and astrocytes—known to respond to stress and GC exposure (Yau, Wheelan, et al. 2015). This integrative approach aimed to uncover the

Summary

- Gut microbiota alpha diversity significantly increased in the ABA mice; the DSOK-0011 group showed an increase in the *Lachnospiraceae* family.
- DSOK-0011 treatment was associated with shifts in wheel-running activity timing, particularly, increased postprandial activity.
- No significant effects were observed on body weight, food intake, or corticosterone levels following DSOK-0011 administration.

potential of 11 β -HSD1 inhibition as a novel therapeutic strategy that targets both neuroendocrine and gut-mediated pathways in AN.

2 | Materials and Methods

2.1 | Animals

For all experiments, female C57BL/6J mice (n = 194, 7 weeks old, referred to as adolescents) were purchased from CLEA Japan Inc., Japan. Depending on the experiment, mice were randomly assigned as follows: 66 for in vivo pharmacokinetics test; 72 for restraint stress model experiment; 56 for ABA model experiment. Mice were housed individually for the ABA model experiment or four to five mice together for other experiments in a controlled environment (temperature, 23°C \pm 0.5°C; relative humidity, 50% \pm 10%) under an inverted 12/12h light-dark cycle (dark phase at 10 a.m. to 10 p.m.). During the study, the animals were fed regular chow (MF diet containing 4.9% fat, Oriental Yeast Co. Ltd., Japan) and had ad libitum access to water. Considering that AN is more prevalent in women than in men, this study was conducted using female mice according to other neuroscience research (van Eeden et al. 2021; Nguyen et al. 2025). All procedures were approved by the Animal Care and Use Committee, Okayama University (approved No. OKU-2023359), and conducted according to the Guidelines for Proper Conduct of Animal Experiments (Science Council of Japan).

2.2 | In Vivo Pharmacokinetics Test

The pharmacological compound DSOK (Lot# R12003) was provided by Sumitomo Pharma Co. Ltd. (Japan) under a material transfer agreement. To evaluate drug pharmacokinetics, DSOK was administered orally (per os, p.o.) to 7-week-old female C57BL/6 mice (n=3 per time point) at doses of DSOK 3, 10, 30, 100, and 1000 mg/kg (see below for the details of preparing suspension). For the pharmacokinetic analysis, blood and brain samples were collected at the following time points: for the 3 mg/kg group, at 0.25, 0.5, 1, 2, 4, and 6 h; and for the 10 mg/kg group, at 0.5, 1, 2, and 4 h. These sampling schedules were designed based on preliminary data to capture dose-specific pharmacokinetic profiles. Mice were initially anesthetized with 2% isoflurane and then deeply anesthetized with 5%, and blood samples were collected from the inferior

vena cava into tubes containing sodium heparin (final heparin concentration: 100 U/mL). Plasma was separated from the whole blood by centrifuging at 3000 rpm. For brain collection, a craniotomy was performed to access the brain, followed by transcardial perfusion with PBS. Brains were immediately dissected after decapitation, weighed, and homogenized in PBS at a ratio of 1:9 (w/v). For quantitative DSOK analysis, plasma and brain homogenates were first deproteinized with methanol. Following centrifugation of the precipitated samples, the supernatants were collected and analyzed by liquid chromatography-tandem mass spectrometry (LC-MS/MS) to determine DSOK concentrations.

2.3 | Preparation of DSOK-0011 Suspensions

A 100 mg/mL master suspension (final volume, 10.0 mL) was prepared by weighing 1.00g of DSOK on an analytical balance, triturating the powder in an agate mortar, and gradually adding sterile 0.5% methyl cellulose 400 (MC; FUJIFILM Wako Pure Chemical Corporation, Japan) with continuous mixing to bring the suspension to 10.0 mL; the mixture was then vortexed for 15 min to ensure homogeneity. From the 100 mg/mL stock, the following working suspensions (10.0 mL each, in 0.5% MC) were prepared: 10 mg/mL, 1.0 mL stock + 9.0 mL MC; 3 mg/ mL, 3.0 mL of the 10 mg/mL suspension + 7.0 mL MC; 1 mg/ mL, 1.0 mL of the 10 mg/mL suspension + 9.0 mL MC; 0.3 mg/ mL, 3.0 mL of the 1 mg/mL suspension + 7.0 mL MC. For the ABA model, a fresh 10 mg/mL DSOK suspension in 0.5% MC was prepared immediately before each daily administration and dosed at 100 mg/kg; per-animal volumes were calculated from body weight and dosing concentration (e.g., 0.155 mL for a 15.5 g mouse).

2.4 | Physical Restraint Stress Model and DSOK-0011 Treatment Experiment

Briefly, we used a mouse model of restraint stress for 1h (n=72) to induce blood corticosterone elevation (Layé et al. 2001; Ding et al. 2021). Four to five mice were housed in individual cages at $22^{\circ}C \pm 2^{\circ}C$ and $50\% \pm 5\%$ relative humidity under an inverted 12/12h light-dark cycle for 5 days. Thereafter, the animals were moved to the experiment room at 10 am and acclimated for 1 h, just before the transition from the light phase to the dark phase (light: 580 lx; dark: 8 lx), followed by DSOK administration (3, 10, or 30 mg/kg, p.o.) or vehicle. After 30 min, a 1 h restraint was performed from 11:30 a.m. in a plastic tube with adequate ventilation holes for preventing excessive movement under the dark conditions, minimizing light-induced corticosterone elevation. At the end, the animals were anesthetized, and blood samples were taken as described above in the method of in vivo pharmacokinetics test.

2.5 | ABA Model and DSOK-0011 Treatment Experiment

ABA mice were individually housed in cages equipped with a running wheel (wheel diameter 23 cm; cat # BIO-ACTIVW-M;

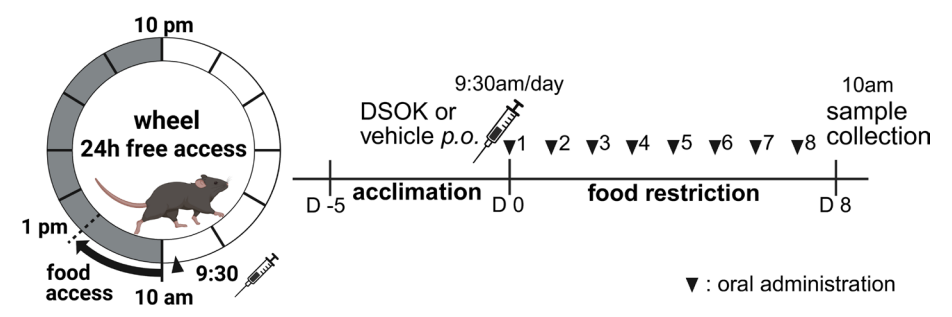


FIGURE 1 | Outline of ABA protocol and drug administration.

Bioseb, France) connected to the Spontaneous Activity Wheel software (Bioseb, France) to continuously record physical activity during the entire protocol (experimental timeline is shown in Figure 1). Notably, the running wheel was freely accessible for 24h a day until the end of the experiment. Body weight and food intake were measured daily at the end of the light phase. We first verified whether ABA mice showed elevated corticosterone levels with increasing severity of body weight loss. Following confirmation of elevated corticosterone levels, an acclimation period for the ABA cohort of the treatment experiment was initiated. After 5 days of acclimation, mice were randomly split into two groups: vehicle or DSOK-0011 (DSOK) group (n = 10 and 11, respectively). Beginning on Day 0, all food was removed from the cage and returned only for 3 h daily (free access to food from 10 a.m. to 1 p.m.). Food intake was recorded at the end of feeding time. Mice in the DSOK group were orally administered the DSOK suspension (dose, 100 mg/kg) at 9:30 a.m., 30 min before the start of the dark phase, once daily for 8 consecutive days (cumulative dose of 800 mg/kg). Mice in the vehicle group received an equal volume of 0.5% MC via a disposable zonde. Animals were removed from the ABA protocol when body weight reduced to less than 75% of the baseline body weight (defined as body weight at the start of the dark phase on Day 0). On Day 8, animals were anesthetized with 2% isoflurane and deeply anesthetized with 5% isoflurane to ensure euthanasia. Blood was collected as described above in the method of in vivo pharmacokinetics test and stored at -80°C until analysis. Following blood collection, transcardial perfusion was performed with phosphatebuffered saline (PBS), and cecal contents were harvested and immediately frozen at -80°C. Then mice were perfused transcardially with 4% of paraformaldehyde (PFA) in PBS for brain fixation and excised. Whole brains were postfixed for 12 h at 4°C, transferred to 30% sucrose solution for 48 h at 4°C for cryoprotection, embedded in Tissue-Tek Optimal Cutting Temperature Compound (Sakura Finetek, Japan), and stored at -80°C until use.

2.6 | Enzyme-Linked Immunosorbent Assay (ELISA) and Fluorometric Assay

Corticosterone levels were measured using a corticosterone enzyme immunoassay kit (cat # ADI-900-097; Enzo Life Sciences, USA). Additionally, cholesterol levels, including high-density lipoprotein (HDL) and low-density and very low-density lipoprotein ratios (LDL/VLDL), were determined using a cholesterol assay kit (cat # ab65390; Abcam, UK). Samples were analyzed

in duplicate via a single fluorometry assay using a Multiskan FC microplate photometer (Thermo Fisher, USA) according to the manufacturer's guidelines.

2.7 | Gut Microbiota Analyses

DNA was extracted from mouse cecal content using the QIAamp Fast DNA Stool Mini Kit (QIAGEN, Japan) according to the manufacturer's manual, with the lysis temperature set to 80°C. DNA libraries were prepared based on hypervariable regions V3-V4 of the 16S rRNA gene. Thereafter, the amplicons were purified, quantified, and sequenced with primers 341F and 805R (Klindworth et al. 2013) by Fasmac Co. Ltd., Japan, using an MiSeq (Illumina, USA). Sequencing was performed using the SILVA 16S rRNA gene reference alignment database, processed using denoising algorithms, and clustered into amplicon sequence variants (ASVs). To identify chimeras in the reads, the nonchimeric 16S rRNA database from QIIME2 (v2023.9) was used. Alpha diversity was assessed using the Shannon and Chao1 indices. Beta diversity was analyzed using Bray-Curtis dissimilarity, weighted and unweighted unique fraction metric (UniFrac) distances.

2.8 | Immunohistochemistry and Image Analysis

Briefly, brain tissue was cut into $30\,\mu m$ sections, permeabilized in 0.2% Triton-X100 in PBS, and blocked with 10% donkey serum (FUJIFILM Wako Pure Chemical Corporation, Japan) for 1 h. Thereafter, the sections were incubated overnight at 4°C with anti-glial fibrillary acidic protein (GFAP) antibody (dilution 1:400; cat # 80788 T, Cell Signaling Technology, USA) for reactive astrocyte staining or anti-ionized calcium binding adapter protein 1 (Iba1) antibody (dilution 1:500; cat # 019-19741, FUJIFILM Wako Pure Chemical Corporation, Japan) for microglia staining. After three washes with PBS (5 min each), the sections were incubated with Alexa Fluor 647 anti-rabbit IgG secondary antibody (dilution 1:400, cat # A32795, Thermo Fisher, USA) at 22°C for 2 h. Finally, DAPI (4',6-diamidino-2-phenylindole) staining was performed using Fluoro-KEEPER Antifade Reagent with DAPI (cat # 12745-74, Nacalai tesque, Japan).

Imaging and quantification were performed, and stained coronal slices were captured using the BZ-X700 All-in-one Fluorescence Microscope (Keyence Corp., Japan). Briefly, the CA1 region of the hippocampus was used as a region of interest (ROI) and analyzed. Each ROI was captured using a $\times 60$ objective lens,

avoiding large blood vessels. To quantify the number of GFAP⁺ and Iba1⁺ cells, we used the "grid" line overlay function in Fiji to randomly place multiple 0.01 mm² subregions in the ROI. We counted only cells following the criteria: (1) positive staining for GFAP or Iba1, (2) clearly visible cell bodies, and (3) identifiable nuclei stained with DAPI. Counting was performed manually using the "multipoint" function in Fiji. The number of cells was calculated as the average counts per mm², according to other studies (Chaaya et al. 2023; Luijerink et al. 2024). This analysis was conducted on three coronal sections per animal, corresponding to bregma levels –1.95 to –2.04 mm. The results were verified by an independent researcher.

2.9 | Statistical Analysis

All data are presented as mean ± standard error of the mean (SEM). The normality of data distributions was assessed using the Shapiro-Wilk test, and all subsequent statistical analyses were conducted using nonparametric methods. The Mann-Whitney U test was applied for comparisons between two independent groups. When comparing three or more groups, the Kruskal-Wallis test and post hoc multiple comparison tests were performed, and p-values were corrected using the Benjamini and Hochberg method to control the false discovery rate (FDR) (Benjamini and Hochberg 1995), with FDR q-values < 0.05 considered statistically significant. The difference in microbial community structure among the groups was tested using permutational multivariate analysis of variance (PERMANOVA) with the "adonis" function in the R "vegan" package with 9999 permutations. Effect sizes are reported as r values (range: 0–1), with values greater than 0.5 typically interpreted as large effects. Correlation analyses were performed using Spearman's rank correlation coefficient reported as r_s . Statistical analysis and graph generation were performed using the R (v4.4.3), GraphPad Prism (v10.4.1), and QIIME2 (v2023.9).

3 | Results

3.1 | DSOK-0011 Suppressed the Plasma Corticosterone Elevation Induced by Physical Restraint Stress

In vivo pharmacokinetic analysis was performed to confirm the safe/effective dose of DSOK in ABA mice. Figure 2A shows the chemical structure of DSOK. First, to examine the peripheral concentration-time profile under minimal systemic exposure, a low-dose test of DSOK (3 mg/kg) was administered (Figure 2B). Following administration, plasma concentration of DSOK peaked within 0.5 h, reaching a maximum concentration (C_{max}) , the highest DSOK concentration observed in the blood) of 711.34 ± 2.12 ng/mL. In addition, a higher dose of DSOK (10 mg/kg) was used to measure total and free concentrations of DSOK in plasma and brain from 0 to 4h postadministration, as this dose was necessary to ensure detectable levels of DSOK in the brain. Total concentration includes both protein-bound and unbound (free) DSOK, while the free concentration represents only the unbound, pharmacologically active form of DSOK. The area under the concentration-time curve from 0 to 4h (AUC $_{0-4h}$, an indicator of overall drug exposure over time)

was 5522.09 ng h/mL and 4347.03 ng h/mL in plasma and brain (Figure 2C). The unbound fractions of DSOK in the serum and brain were 0.032 and 0.016, respectively, indicating high protein binding efficiencies (96.8% in serum and 98.4% in brain). The unbound brain-to-plasma partition coefficient ($K_{\rm p,uu,brain}$, which reflects the extent to which the free drug distributes into the brain) (Gupta et al. 2006) ranged from 0.35 to 0.42. To assess the pharmacodynamic efficacy of DSOK, we evaluated its ability to suppress plasma corticosterone levels in a physical restraint stress model (Figure 2D). DSOK dose-dependently reduced corticosterone levels, confirming its in vivo activity as a corticosterone suppressor. The effect sizes compared to the vehicle group were 0.801 (30 mg/kg), 0.530 (10 mg/kg), and 0.218 (3 mg/kg), respectively. To evaluate the duration for which DSOK remains in systemic circulation, we next examined the time course of its plasma concentration (Figure 2E). After a 30 mg/kg dose, DSOK was almost completely cleared from the plasma within 24h. Based on these results, we confirmed the optimal dose for ABA mice and estimated the duration over which DSOK maintains a total plasma concentration of 159 ng/mL, corresponding to its in vitro half-maximal inhibitory concentration (IC₅₀, the concentration at which the drug inhibits 50% of 11\beta-HSD1 activity) of 4.8 nM. According to simulation data (not shown), the effective plasma concentration of DSOK can be sustained for approximately 9 and 16h with doses of 30 and 100 mg/kg, respectively. Taken together with the pharmacokinetic and pharmacodynamic data, a twice-daily administration of 30 mg/kg would be expected to maintain therapeutic levels (as shown in Figure 2D,E). However, to minimize the stress associated with repeated dosing in animals, a once-daily administration of 100 mg/kg was selected for the ABA mouse model.

3.2 | DSOK-0011 Affects Daily Activity Patterns, but Does Not Prevent Exercise-Induced Body Weight Loss

To evaluate the effects of DSOK in the ABA mouse model, we assessed body weight, food intake, and physical activity patterns. Plasma corticosterone levels were significantly elevated in the ABA mice compared to controls (p = 0.0002, effect size (r) = 0.699) (Figure 3A), and this increase was correlated with the percentage of body weight loss (Spearman's rank correlation coefficient $(r_s) = -0.52$, p = 0.0474) (Figure 3B). We next examined the effects of DSOK on activity rhythms. Compared to the vehicle-treated mice, DSOK-treated mice showed a significant reduction in mean hourly running distance during the penultimate hour before food access (9 a.m.-10 a.m.), corresponding to food anticipatory activity (FAA), and a significant increase in activity 6h after the onset of the dark phase (Figure 3C). During the early phase of the ABA paradigm (Days 0 and 1), the DSOK group exhibited significantly higher mean activity during the dark phase, whereas the vehicle group showed a significant increase in activity during the light phase (Figure 3D). Although these group differences were not statistically significant on subsequent days, DSOKtreated mice tended to show consistently higher mean daily activity levels throughout the rest of the ABA period. To further characterize these trends, we analyzed running activity separately for the light phase, dark phase, and FAA (3 h before food access) across Days 1-7 of the ABA period (Figure 3E).

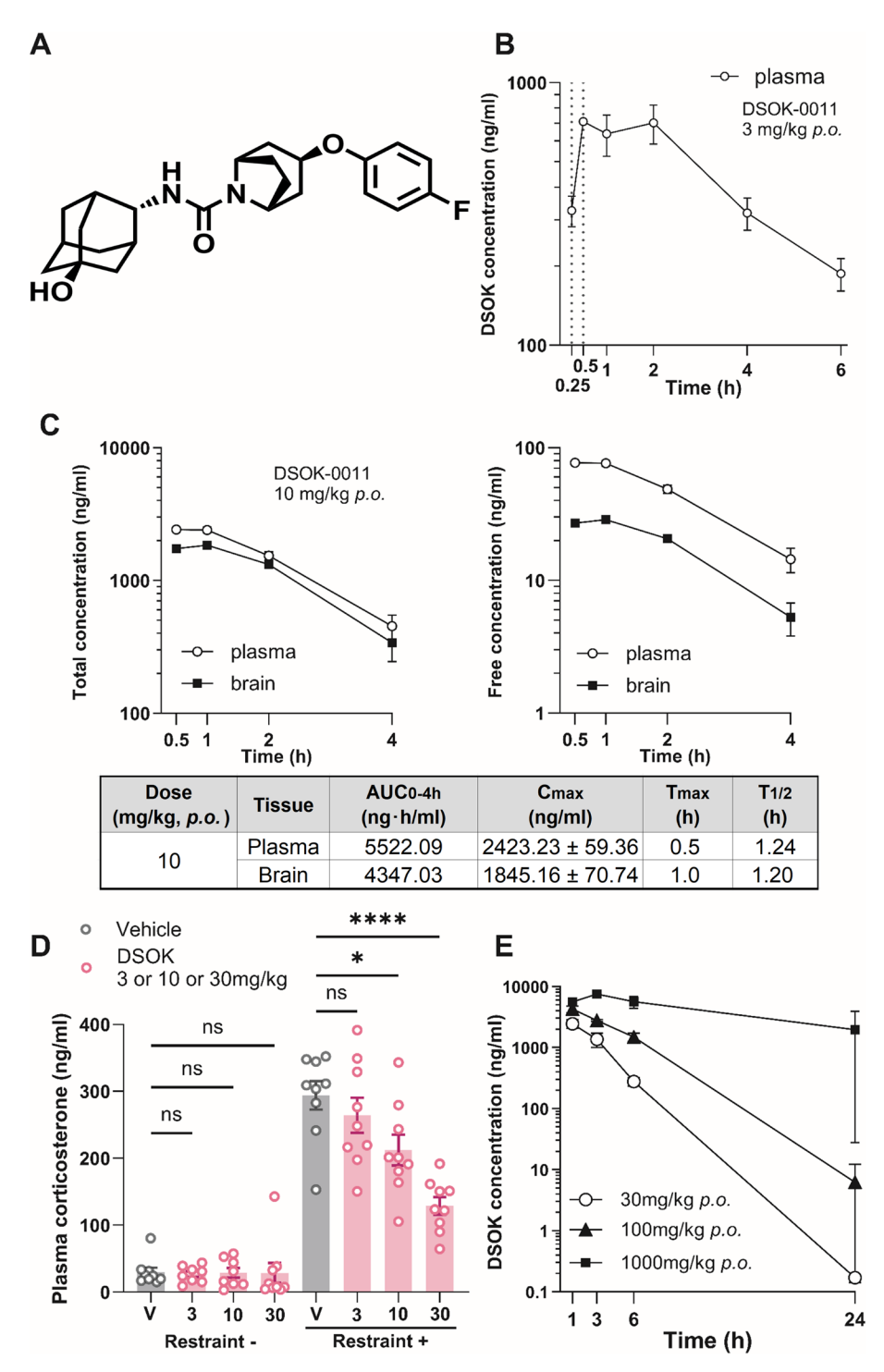


FIGURE 2 | DSOK-0011 pharmacological profiles and its effect on plasma corticosterone in a mouse model of physical restraint stress. (A) Chemical structure of DSOK-0011. (B) Total plasma concentration of DSOK following oral administration of 3 mg/kg over a 6 h period. The y axis is presented on a logarithmic (\log_{10}) scale. (C) Total and free concentrations of DSOK in plasma and brain following oral administration of 10 mg/kg. Pharmacokinetic parameters include area under the concentration-time curve from 0 to 4 h (AUC_{0-4h}), maximum observed concentration (C_{max}), time to reach C_{max} (T_{max}), and plasma half-life ($T_{1/2}$). The y axis is presented on a logarithmic (\log_{10}) scale. (D) Plasma corticosterone concentrations in mice with or without physical restraint stress, treated with vehicle (V) or DSOK at 3, 10, or 30 mg/kg (p.o.). Values are reported as mean \pm SEM (ng/mL) as follows: Without (–) restraint: V, 29.79 ± 6.65 ; 3 mg/kg, 26.75 ± 4.29 ; 10 mg/kg, 28.67 ± 7.33 ; 30 mg/kg, 28.57 ± 14.88 . With (+) restraint: V, 293.99 ± 21.12 ; 3 mg/kg, 264.32 ± 26.26 ; 10 mg/kg, 212.20 ± 22.99 ; 30 mg/kg, 128.73 ± 13.08 . Each group consisted of n=9 mice, except the 3 mg/kg no-restraint group (n=8) due to one value falling below the detectable range. Effect sizes (r) for comparisons with the vehicle group under restraint were as follows: 3 mg/kg, r=0.218; 10 mg/kg, r=0.530; 30 mg/kg, r=0.801. Kruskal-Wallis test with the FDR correction, adjusted p-values are shown (ns: not significant, *p=0.0204; ******p<0.0001). (E) Plasma concentration profile of DSOK over 24h following oral administration of 30, 100, or 1000 mg/kg. The y axis is presented on a logarithmic (\log_{10}) scale. All data are presented as mean \pm standard error of the mean (SEM).

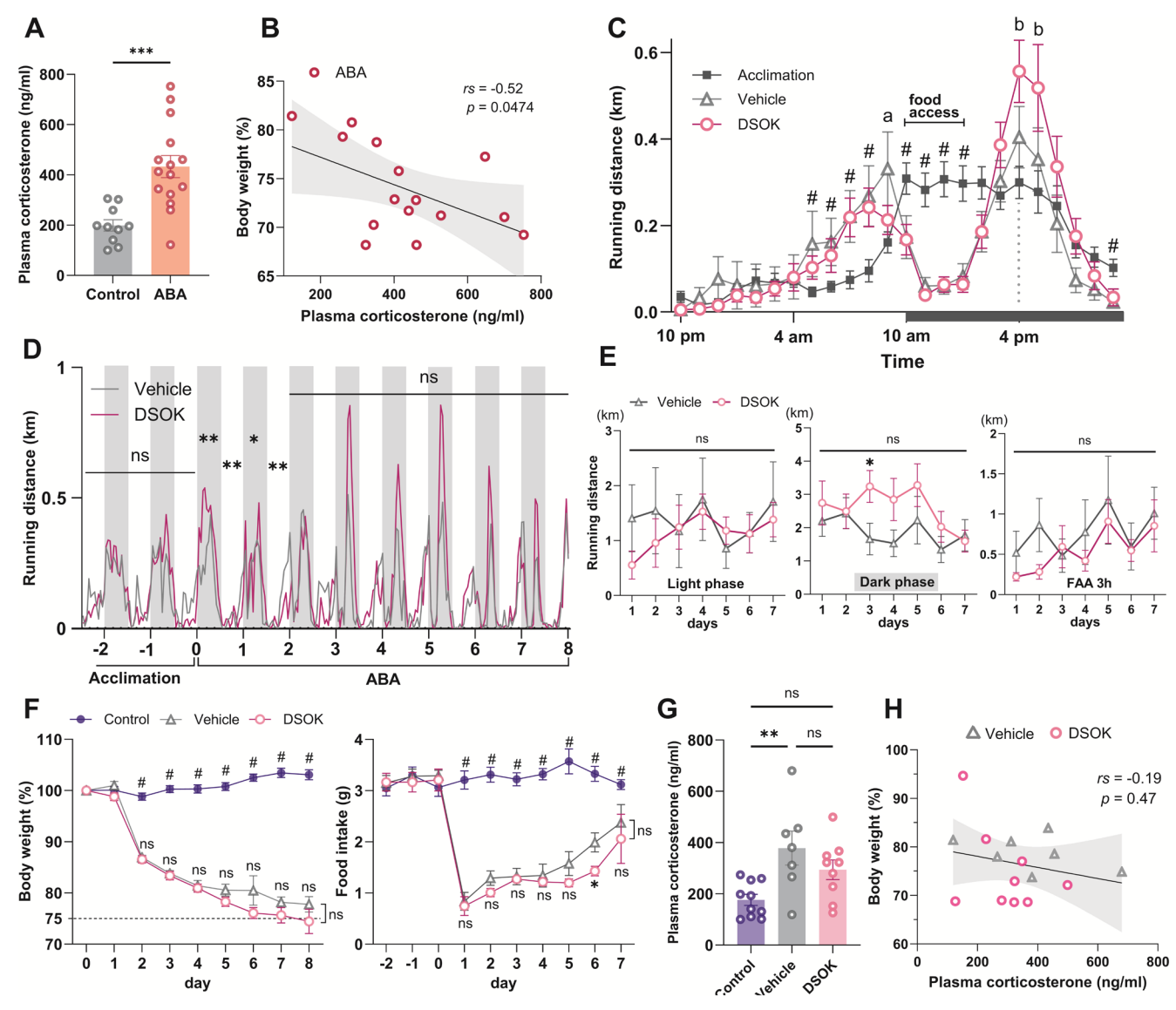


FIGURE 3 | Effects of 11β-HSD1 inhibitor DSOK-0011 on body weight, food consumption, and physical activity in ABA mice. (A) Plasma corticosterone levels in control and ABA groups (n=10 and 15, respectively; control: 173.25±20.62 ng/mL; ABA: 439.38±47.76 ng/mL). ***p=0.0002; effect size r=0.699. (B) Correlation between plasma corticosterone levels and body weight in ABA mice. Line represents linear regression with 95% confidence band. Spearman's correlation coefficient (r_s)=-0.52, p=0.0474. (C) Diurnal activity patterns of vehicle- and DSOK-treated mice during ABA. Acclimation phase activity used as baseline (n=10 and 11). #Significant difference versus baseline, p<0.05; a, vehicle group versus baseline, p=0.0229; b, DSOK group versus baseline; 4p.m.-5p.m., p=0.018; 5p.m.-6p.m., p=0.043. (D) Mean activity levels during ABA period in vehicle and DSOK groups (n=10 and 11, gray bars indicate dark phase). Day 0: Dark phase, p=0.0029; light phase, p=0.0018; Day 1: Dark phase, p=0.010; light phase, p=0.0083. ns: not significant. (E) Activity levels in light phase, dark phase, and FAA (3h before feeding) on Days 1-7. Significant increase in dark phase activity on Day 3 in DSOK group (p=0.031). (F) Body weight and food intake changes during ABA in control, vehicle, and DSOK groups (n=10, 10, and 11, respectively). #DSOK and vehicle versus control, p<0.001; *vehicle versus DSOK. Day 6, p=0.022. (G) Plasma corticosterone levels in the control, vehicle, and DSOK groups (n=10, 7, and 9; control: 167.22±21.93 ng/mL, vehicle: 378.48±66.25 ng/mL, DSOK: 294.11±38.17 ng/mL). **p=0.0065; effect sizes (p): control versus vehicle, p=0.639; control versus DSOK, p=0.56; Vehicle versus DSOK, p=0.224. (H) Correlation between plasma corticosterone levels and body weight in vehicle and DSOK groups: p=0.47. Statistical analysis: (A, C-F): Mann-Whitney p=0.0065; Effect sizes (p=0.0065; Control versus vehicle versus DSOK groups: p=0.47. Statistical analysis: (A, C-F): Mann-Whitney

No significant differences were observed between the DSOK and vehicle groups on most days across these time periods; however, dark-phase activity was significantly elevated in the DSOK group on Day 3 (p = 0.031). As shown in Figure 3F, both vehicle- and DSOK-treated groups showed significant reductions in body weight compared to the control group during the ABA period. However, no significant difference

in body weight loss was observed between the vehicle and DSOK groups (Figure 3F, left). Similarly, food intake was significantly reduced in both groups compared to controls, with no significant differences between the vehicle and DSOK groups throughout most of the experimental period, except on Day 6, when the DSOK group consumed significantly less food (p = 0.022) (Figure 3F, right). During the ABA period, 7

out of 11 DSOK-treated mice and 5 out of 10 vehicle-treated mice met the dropout criterion due to > 25% body weight loss. However, there was no statistically significant difference in dropout rates between the groups (Log-rank test: $\chi^2 = 1.060$, p = 0.303). Among the three groups, plasma corticosterone levels were significantly higher in the vehicle group compared to controls (p = 0.0065; r = 0.639). Although corticosterone levels were numerically elevated in the DSOK group relative to controls (r = 0.561), this difference did not reach statistical significance. Likewise, no significant difference was observed between the vehicle and DSOK groups (r = 0.224) (Figure 3G). Finally, we examined potential associations between plasma corticosterone levels and body weight; no significant correlations were identified (Figure 3H). In summary, DSOK treatment did not significantly affect body weight, food intake, or plasma corticosterone levels in ABA mice. However, DSOK potentially modulates daily activity rhythms, particularly by increasing postprandial activity and reducing FAA in the certain times during the early phase of treatment.

3.3 | Effect of DSOK-0011 Treatment on the Gut Microbiota in ABA Mice

To assess the impact of DSOK on the gut bacteria, we analyzed the microbiota alterations in vehicle- or DSOK-treated ABA mice compared to the control group. The composition of gut microbiota at both the family and genus levels was presented using stacked bar plots, displaying the top 10 most abundant taxa based on relative abundance in control mice (Figure 4A). Taxa with < 1% relative abundance were grouped as "Others," and unidentified bacteria were labeled as "Unclassified." Notably, the relative abundance of the Lachnospiraceae family showed a stepwise increase across the groups (Figure 4B left). While the difference between the control and vehicle groups was not statistically significant (p = 0.106, effect size r=0.44), a significant increase was observed in the DSOK group (vs. control: p = 0.0004, r = 0.82; vs. vehicle: p = 0.05, r = 0.54). Consistent with this result, a genus-level analysis of Lachnospiraceae_NK4A136_group also significantly increased in the DSOK group (control vs. DSOK: p = 0.0001, r=0.82; vehicle vs. DSOK: p=0.05, r=0.54; control vs. vehicle: p = 0.12, r = 0.42), but no other genera belonging to the Lachnospiraceae family showed significant differences. Conversely, the Anaerovoracaceae family showed a stepwise decrease across the groups (Figure 4B right). Although the reduction from control to vehicle was not statistically significant (p=0.244, r=0.4), the abundance was significantly lower in the DSOK group compared to other groups (vs. control: p = 0.0003, r = 0.73; vs. vehicle: p = 0.029, r = 0.67). These findings suggest that the bidirectional changes in Lachnospiraceae and Anaerovoracaceae reflect treatment-dependent modulation of specific microbial taxa in ABA mice. Furthermore, we conducted the differential abundance analysis based on log, fold change to broadly assess changes in ABA mice compared to controls (Figure 4C, left: vehicle; right: DSOK; presented families shown FDR-corrected p < 0.05). Several families, including Lachnospiraceae and Anaerovoracaceae, exhibited significant changes in both ABA groups, indicating a potential microbial response to ABA-induced FR and/or physical activity. Moreover, to assess alpha diversity (within-sample), we calculated the Shannon and Chao1 indices (Figure 4D). Both indices were significantly higher in the vehicle and DSOK groups compared to controls (Shannon: vehicle, p = 0.012; DSOK, p < 0.0001; Chao1: vehicle, p = 0.001; DSOK, p = 0.018), suggesting increased microbial richness and evenness. However, no significant differences were observed between the vehicle and DSOK groups for either index. This contrasts with previous studies, which have reported either no change or only slight increases in alpha diversity in patients with AN (Di Lodovico et al. 2021; Yuan et al. 2022), and similarly in ABA rodent models (Breton et al. 2021; Trinh et al. 2021). This discrepancy suggests that the oral administration of vehicle or DSOK may have influenced microbial diversity independently of the ABA condition. Beta diversity (between-sample) was evaluated using principal coordinate analysis (PCoA) based on UniFrac distances (Figure 4E). PERMANOVA with Bray-Curtis dissimilarity and weighted UniFrac distances (Figure 4E left and center) revealed significant separation between the controls and both ABA groups (Bray-Curtis: vs. vehicle, p = 0.0001, F = 11.37, $R^2 = 0.43$; vs. DSOK, p = 0.0001, F = 15.98, $R^2 = 0.48$; weighted UniFrac: vs. vehicle, p = 0.001, $F = 31.41, R^2 = 0.67$; vs. DSOK, $p = 0.001, F = 46.58, R^2 = 0.73$), but no significant difference between the vehicle and DSOK groups (Bray-Curtis: p = 0.092, F = 1.34, $R^2 = 0.087$; weighted UniFrac: p = 0.095, F = 2.22, $R^2 = 0.13$). In contrast, unweighted UniFrac distances showed significant differences among all groups (control vs. vehicle: p = 0.0001, F = 5.57, $R^2 = 0.27$; control vs. DSOK, p = 0.0001, F = 7.45, $R^2 = 0.30$; vehicle vs. DSOK, p = 0.038, F = 1.42, $R^2 = 0.092$). These findings suggest that while the ABA paradigm could alter the overall community structure, DSOK treatment further altered the composition of low-abundance or rare taxa. Finally, we examined whether the two bacterial families that showed significant differences between the vehicle and DSOK groups, Lachnospiraceae and Anaerovoracaceae, were associated with plasma corticosterone levels. Lachnospiraceae abundance positively correlated with corticosterone levels (Spearman's $r_c = 0.433$, p = 0.027; Figure 4F), whereas Anaerovoracaceae showed no significant correlation ($r_s = -0.2$, p = 0.307; data not shown). These results suggest that Lachnospiraceae may play a role in promoting corticosterone synthesis, potentially via the 11β-HSD1 activity under ABA conditions.

3.4 | DSOK-0011 Has No Effect on Plasma Cholesterol Levels in ABA Mice

Although studies on HDL and LDL levels in the ABA model remain limited, 11β -HSD inhibition has been shown to improve lipid profiles in metabolic disorders, indicating that this enzyme may be a potential therapeutic target for dyslipidemia (Hu et al. 2013; Berthiaume et al. 2007). To investigate the effect of DSOK on lipid profile in ABA mice, we examined plasma cholesterol levels, focusing on HDL levels and the LDL/VLDL ratio. Compared with those in the control group, there was a decrease in plasma total cholesterol level in the vehicle group (Figure 5A) and a significant decrease in HDL levels in the vehicle and DSOK groups (Figure 5B). In contrast, there were no significant differences in LDL/VLDL ratios among the groups (Figure 5C). Furthermore, we found no significant correlations between body weight and cholesterol levels in vehicle-

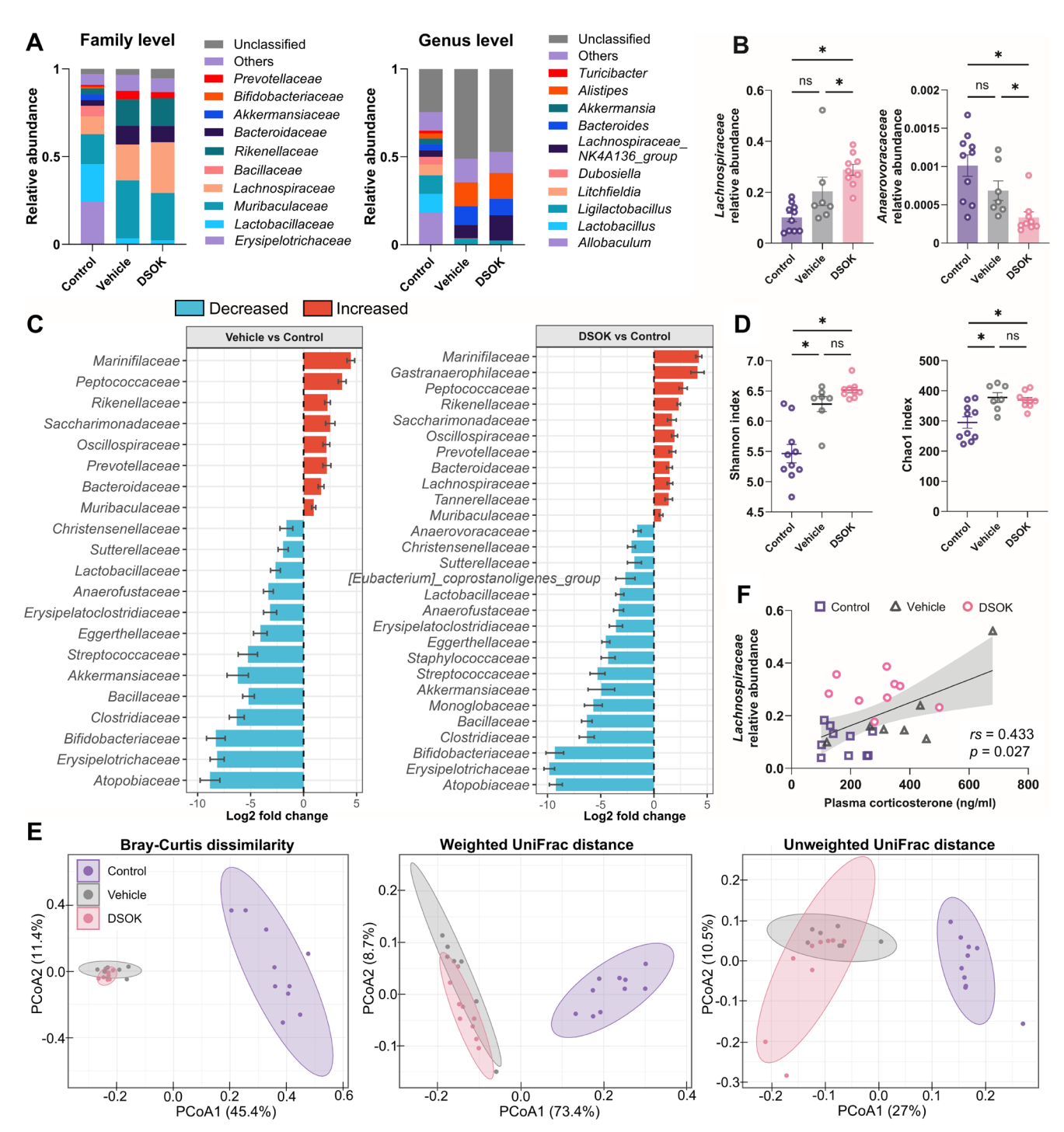


FIGURE 4 | Effects of DSOK-0011 treatment on gut microbiota composition in ABA mice. (A) Stacked bar plots of the mean relative abundance of the Top 10 bacterial taxa at the family and genus levels of control, vehicle, and DSOK groups (n = 10, 7, and 9). (B) Comparisons of relative abundances of *Lachnospiraceae* and *Anaroevocaraceae* families between control, vehicle, and DSOK groups (n = 10, 7, and 9; *p < 0.05, Kraskal-Wallis test with FDR correction). (C) Differential abundance analysis of bacterial families between control (n = 10) and ABA (vehicle on the left, n = 7; DSOK on the right, n = 9). \log_2 fold change was calculated based on the control group's relative abundance. Only taxa with FDR-corrected p < 0.05 are shown. (D) Alpha diversity calculated by Shannon and Chao1 indices between control, vehicle, and DSOK groups (n = 10, 7, and 9; *p < 0.05, Kraskal-Wallis test with FDR correction). (E) Beta diversity of control, vehicle, and DSOK groups (n = 10, 7, and 9). PCoA with Bray-Curtis dissimilarity (left): control versus vehicle, p = 0.0001, F = 11.37, $R^2 = 0.43$; control versus DSOK, p = 0.0001, F = 15.98, $R^2 = 0.48$; vehicle versus DSOK, p = 0.092, F = 1.34, $R^2 = 0.087$; weighted UniFrac distance (center): control versus vehicle, p = 0.001, F = 31.41, p = 0.67; control versus DSOK, p = 0.001, p = 0.00

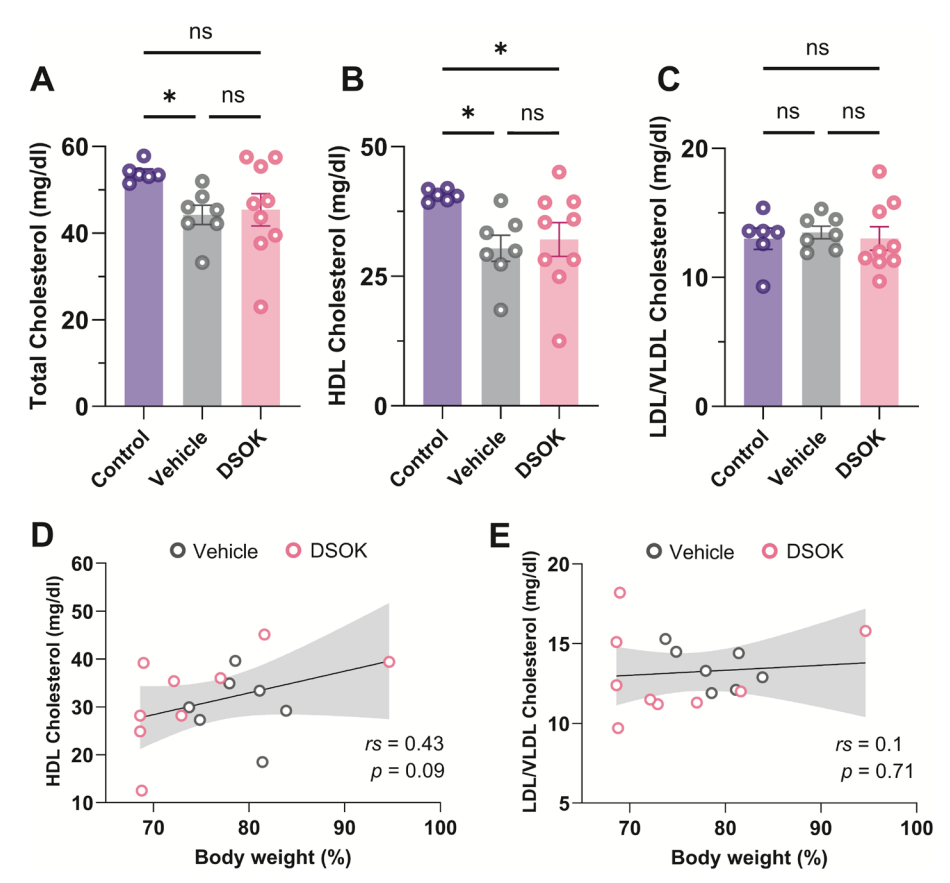


FIGURE 5 | Plasma cholesterol levels in control and ABA mice. (A, B, C) Total cholesterol: control: $53.65 \pm 0.85 \, \text{mg/dL}$, vehicle: $43.88 \pm 2.23 \, \text{mg/dL}$, DSOK: $45.12 \pm 3.77 \, \text{mg/dL}$; *p = 0.0461; effect size (r): control versus vehicle: r = 0.79, versus DSOK: r = 0.36, vehicle versus DSOK: r = 0.11, (A); HDL: control: $40.65 \pm 0.45 \, \text{mg/dL}$, vehicle: $30.4 \pm 2.52 \, \text{mg/dL}$, DSOK: $32.1 \pm 3.26 \, \text{mg/dL}$; control versus vehicle; p = 0.0157; control versus DSOK; p = 0.0476; effect size (r): control versus vehicle: r = 0.79, versus DSOK: r = 0.59, vehicle versus DSOK: r = 0.12, (B); and LDL/VLDL: control: $13.0 \pm 0.82 \, \text{mg/dL}$, vehicle: $13.48 \pm 0.48 \, \text{mg/dL}$, DSOK: $13.02 \pm 0.91 \, \text{mg/dL}$, all data are ns; effect size (r): control versus vehicle: r = 0.1, versus DSOK: r = 0.12, vehicle versus DSOK: r = 0.22, (C); n = 6, n = 6, and n = 6 respectively, Kruskal–Wallis test with FDR correction. (D, E) Correlations between body weight and HDL; Spearman's correlation coefficient (r_s) = 0.43, p = 0.09, (D) and LDL/VLDL; $r_s = 0.1$, p = 0.71, (E). All data are presented as mean \pm standard error of mean (SEM).

DSOK-treated ABA mice (Figure 5D,E). Overall, these results indicate that DSOK may not significantly alter lipid metabolism in mice with ABA.

3.5 | Glial Cells in the CA1 Region of DSOK-0011and Vehicle-Treated ABA Mice

Recent evidence suggests that glial cells may play an important role in the regulation of feeding behavior associated with AN (Frintrop et al. 2021). In the ABA model, structural and functional alterations have been observed in the hippocampus, accompanied by reduced expression of GC receptors (Mottarlini et al. 2024). Moreover, changes in both astrocytes and microglia have been reported under anorexic conditions, including the ABA model, highlighting the potential involvement of glial cells in the neuropathology of AN (Reyes-Haro et al. 2016; Ragu-Varman et al. 2019). Despite these findings, the impact of 11β -HSD1 inhibition, a key regulator of local GC regeneration, on glial cell populations in the hippocampus under the ABA paradigm has not been investigated. Given that 11β -HSD1 is abundantly expressed in the hippocampus (Yau, Noble, et al. 2015; Yau, Wheelan, et al. 2015),

particularly in the dorsal CA1 region, and contributes to both diurnal and stress-induced increases in hippocampal corticosterone levels (Yau, Noble, et al. 2015), we focused our analysis on glial cell populations in this region. To address this gap, we examined the glial cells in the dorsal CA1 region using immunohistochemistry (Figure 6A, bregma -1.95 to $-2.04\,\mathrm{mm}$). Notably, there were no significant differences in the number of GFAP-positive astrocytes (vehicle: $375\pm20\,\mathrm{cells/mm^2}$, DSOK: $435\pm32\,\mathrm{cells/mm^2}$) and Iba1-positive microglia (vehicle: $230\pm16\,\mathrm{cells/mm^2}$, DSOK: $237\pm21\,\mathrm{cells/mm^2}$) in the CA1 regions between the vehicle and DSOK groups (Figure 6B–E). Overall, these results suggest that DSOK administration does not significantly affect glial cell populations in mice with ABA.

4 | Discussion

In this study, we investigated the effects of DSOK-mediated 11β -HSD1 inhibition on physical parameters, circulating GC and lipid regulation, hippocampal glial cells, and gut microbiota composition in ABA mice. Although DSOK did not significantly prevent exercise-induced weight loss, it affected physical

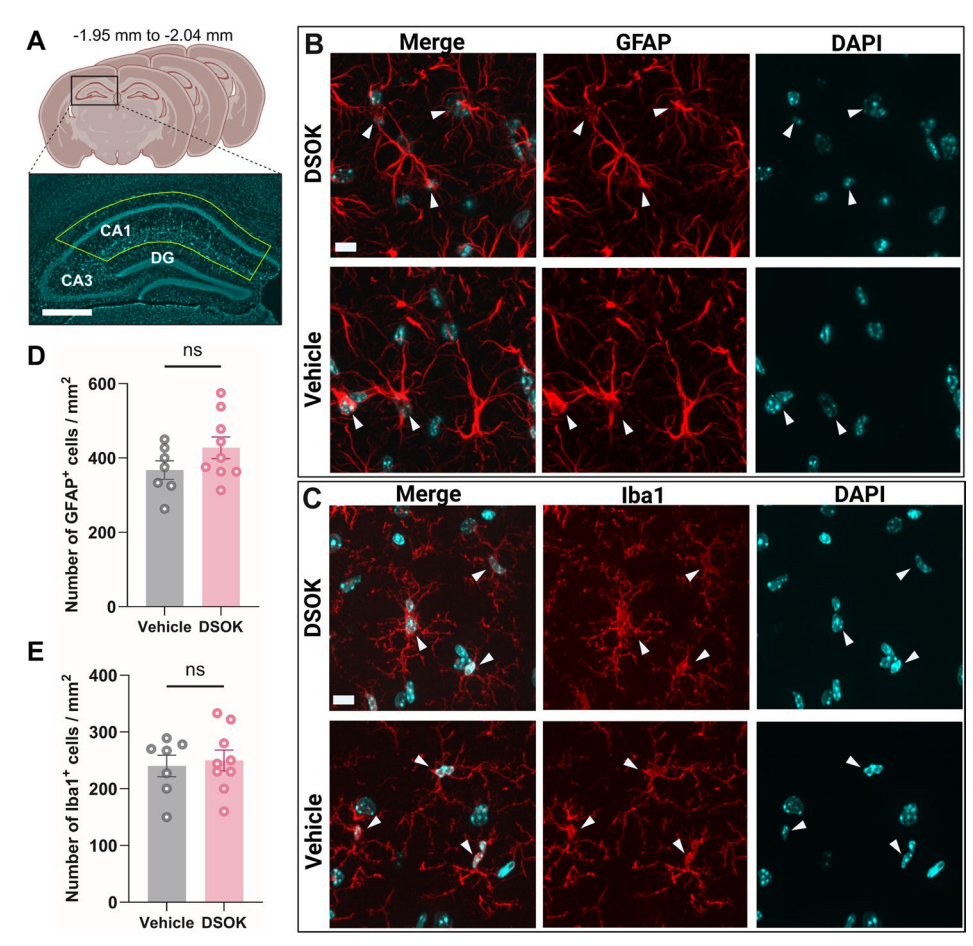


FIGURE 6 | Glial cell population in the CA1 regions of mice in the DSOK and vehicle groups. (A) Yellow line area indicates DAPI (cyan)-stained hippocampal CA1 region, at bregma -1.95 to -2.04 mm. White scale bar indicates $500 \,\mu$ m. (B, C) Each picture showed $1 \,\mathrm{mm}^2$ of the representative region of the CA1. The images were labeled with anti-GFAP antibody (red) and DAPI (cyan) (B) or anti-Iba1 antibody (red) and DAPI (cyan) (C). Arrowheads indicate counted cells. White scale bar indicates $10 \,\mu$ m. (D, E) The number of GFAP+ cells (ns; p = 0.288) (D) and Iba1+ cells (ns; p = 0.776) (E) between vehicle and DSOK group (n = 7 and 9, respectively) in the CA1 region. Statistical analysis: Mann–Whitney U test. Data are presented as mean \pm standard error of mean (SEM).

activity at specific time points of pre- and postprandial periods. Additionally, DSOK administration significantly altered specific intestinal bacteria and alpha diversity.

The selective inhibition of 11β-HSD1 via DSOK treatment may produce a paradoxical interplay between metabolic and behavioral effects in ABA. Chronic caloric restriction and excessive exercise are known to dysregulate the HPA axis (Doerr et al. 1980; Schweitzer et al. 1990; Duclos et al. 2005). In this study, the persistence of ABA-induced corticosterone elevation despite inhibiting its regeneration via 11β-HSD1 suggests that central HPA axis drivers such as CRH and arginine vasopressin may override peripheral mechanisms or elicit compensatory upregulations. Conversely, the absence of changes in circulating corticosterone levels (Figure 3H) without any adjustments in food intake or weight loss (Figure 3F) suggests that elevated corticosterone levels were not accompanied by the upregulation of CRH, a potent anorexigenic factor (Glowa et al. 1992). Consistent with previous findings in metabolic diseases (Berthiaume et al. 2007; Courtney et al. 2008; Hermanowski-Vosatka et al. 2005), our study showed that pharmacological inhibition of 11β-HSD1 may function as a potential stabilizer without activating the HPA axis.

In addition, DSOK-treated mice exhibited altered activity patterns. Specifically, there was a significant decrease in wheelrunning activity in the penultimate hour preceding feeding in the DSOK group (Figure 3C). This behavior, commonly referred to as FAA, is a hallmark of rodents under scheduled-FR paradigms such as ABA. In rodents, corticosterone secretion basically follows circadian rhythms regulated by the suprachiasmatic nucleus (SCN), peaking at the transition from the light (rest) phase to the dark (active) phase (Mohawk et al. 2007; Windle et al. 1998). However, scheduled-FR can decouple the corticosterone rhythms from the light-dark cycle and synchronize them with the feeding cycle (Sheward et al. 2007; Namvar et al. 2016; Patton and Mistlberger 2013). GC may play a dual role in FAA: while it facilitates energy-sensing and dopaminergic signaling pathways (González-Vila et al. 2023; de Lartigue and McDougle 2019; Yoshimura et al. 2023), it can also disrupt behavioral rhythms depending on circadian context (Namvar et al. 2016; Silver and Balsam 2010). Dulcos et al. revealed that FAA was lost in adrenalectomized ABA rats, whereas preprandial acute corticosterone injection further increased plasma FAA levels in a concentration-dependent manner, underpinning a strong relationship between them (Duclos et al. 2009). Overall, the observed relationship between FAA and feeding behavior

may partly explain the reduced food intake in the DSOK group on Day 6. However, no significant difference was observed between groups during the light phase on Day 5 (Figure 3E). While average activity during the entire dark phase did not differ between groups (data not shown), DSOK-treated mice exhibited a marked increase in physical activity during postprandial hours (Figure 3C,E). A recent study indicates that elevated activity during the light phase in ABA mice is associated with greater weight loss (Aston et al. 2023). As circadian misalignment exacerbates energy deficits, increased activity during the dark phase, when rodents are naturally active, might be less detrimental to their natural metabolic state. DSOK-treated mice might have shown a partial attenuation of energy wasting, as suggested by lower corticosterone levels compared to the vehicle group (Figure 3G). However, this physiological adjustment did not translate into changes in cholesterol levels (Figure 5A-C), possibly because catabolic processes under severe energy deficit override the lipid-modulatory effects of 11β-HSD1 inhibition. This is consistent with previous findings that the metabolic efficacy of 11β-HSD1 inhibitors is highly dependent on nutritional and hormonal context (Loerz et al. 2017).

Gut microbiota analysis revealed notable alterations in microbial composition in ABA mice. Specifically, we observed a significant increase in the relative abundance of the Lachnospiraceae family after DSOK administration. Although previous studies have implied that gut microbiota and GC metabolism are linked via 11β-HSD1 activity, causal relationships remain unclear (Johnson et al. 2016). Lachnospiraceae, a family within the Firmicutes phylum, has been reported to fluctuate in GCrelated metabolic disorders such as Cushing's syndrome (Zhang, Guan, et al. 2024; Zhang, Shi, et al. 2024). Notably, a previous study using the ABA mice reported no significant change in Lachnospiraceae abundance (Breton et al. 2021). Conversely, our results demonstrated a significant increase in this family in DSOK-treated ABA mice compared to both control and vehicle groups (Figure 4B), with a positive correlation to plasma corticosterone levels (Figure 4F). These findings suggest that Lachnospiraceae may play a role in peripheral corticosterone synthesis through 11β-HSD1-dependent mechanisms (Zhang, Guan, et al. 2024; Zhang, Shi, et al. 2024). Interestingly, the genus Lachnospiraceae_NK4A136_group, a member of this family, has been reported to decrease in GC-induced glycolipid metabolism disorders (Zhang, Guan, et al. 2024). In our study, however, this genus was significantly increased in both vehicle- and DSOK-treated ABA mice. This divergence suggests that under conditions of starvation and excessive physical activity, hallmarks of the ABA model, its response may differ from that observed in overnutrition or GC-induced metabolic dysfunction. These contrasting patterns may highlight the contextdependent nature of GC-responsive microbiota. In addition to taxonomic shifts, we observed changes in microbial diversity. Both Shannon and Chao1 indices were significantly increased in ABA mice compared to controls. This contrasts with previous studies reporting minimal or no changes in alpha diversity in AN patients or ABA models (Breton et al. 2021; Andreani et al. 2024; Schulz et al. 2021). However, a study by Kooij et al. revealed that alpha diversity gradually increased in ABA rats following fecal microbiota transplantation from AN patients (Kooij et al. 2025), suggesting that gut microbial richness may shift in response to nutritional status and/or physical activity.

The increase in the Chaol index, alongside significant shifts in beta diversity (Figure 4D,E), indicates an expansion of lowabundance or rare taxa under ABA conditions. This may reflect microbial adaptation to severe caloric restriction, which alters nutrient availability in the gut. Nonetheless, procedural factors, including the oral gavage of MC as vehicle or DSOK suspension, may independently influence gut microbial diversity. Such variables, along with dietary differences, could account for discrepancies between our findings and previous other studies (Breton et al. 2021; Andreani et al. 2024; Schulz et al. 2021). While our data suggest that DSOK may modulate specific microbial taxa, potentially through inhibition of 11β-HSD1, the causal relationships among DSOK treatment, GC metabolism, and gut microbiota composition have yet to be fully elucidated. To our knowledge, no studies have specifically examined the effects of chronic ABA exposure on gut microbial diversity. The increased alpha diversity observed here might represent an adaptive response of the microbiota to severe caloric restriction and hyperactivity. Our findings, therefore, suggest that DSOK may influence microbial composition through GC-regulated immune and bile acid pathways. However, whether these microbial changes facilitate or impair physiological adaptation to the combined stresses of the acute ABA model, including starvation and circadian disruption, remains unresolved.

Furthermore, no significant changes were observed in astrocytes and microglia population in the CA1 region after 1 week of FR in ABA mice (Figure 6D,E). GC has been shown to affect glial cells in response to various neuroinflammatory factors (Jauregui-Huerta et al. 2010). Particularly, the hippocampus is sensitive and vulnerable to fluctuations in corticosterone level (Zhang et al. 2015; Moisan et al. 1990; Bridges et al. 2008; Saavedra et al. 2018). Previous studies have demonstrated that acute-ABA with 7 days FR does not always lead to marked changes in glial cells; however, the chronic-ABA paradigm with over 2 weeks FR affects the corpus callosum and SCN (Zimmermann et al. 2023, 2025). Our findings suggest that glial cells in the CA1 region might exhibit resilience or delayed responses to short-term starvation stress, potentially reflecting the transient nature or a protective adaptation to maintain the central homeostasis during the early phase of ABA. Overall, it is crucial to investigate the effects of 11β-HSD1 inhibition on GC metabolism in brain glial cells using a chronic ABA paradigm.

In conclusion, our findings provide valuable preclinical insights into the role of GC metabolism in AN pathophysiology, potentially mediated by the 11β-HSD1. DSOK may exert protective effects against ABA-induced stress and inflammation. However, we did not directly confirm the in vivo inhibition of 11β -HSD1 activity in the ABA model, so the involvement of this enzyme should be interpreted with caution. Elevated GC levels in AN or ABA may reflect an adaptive response to starvation, which could explain the limited success of pharmacological approaches targeting peripheral GC synthesis. Corticosterone levels are highly variable, influenced by circadian rhythms, estrous cycles (Atkinson and Waddell 1997), daily handling, and individual differences in HPA axis reactivity, thereby complicating the data interpretation. These factors likely contributed to interindividual and intergroup differences observed in corticosterone concentrations. Additionally, our study is limited by a small sample size and uncertainty regarding optimal dosing

and administration timing. Lack of data on different doses (e.g., 100 mg/kg dose of DSOK in the restraint stress model and 30 mg/kg dose of DSOK in the ABA model) was also a limitation of this study. Although DSOK reduced corticosterone in acute restraint stress, this may not fully translate to its effects in the 7-day ABA model. Therefore, the in vivo corticosterone-suppressing efficacy of DSOK must be interpreted with caution. Given our findings that DSOK does not appear to trigger compensatory HPA axis activation, further research is warranted.

Author Contributions

Hiroki Kawai: conceptualization, methodology, software, data curation, formal analysis, investigation, project administration, visualization, funding acquisition, writing - original draft, validation, resources. Nanami Wada: formal analysis, data curation, visualization, investigation, validation. Shinji Sakamoto: conceptualization, investigation, methodology, validation, project administration, funding acquisition, writing - review and editing, data curation. Kenji Miyazaki: investigation, data curation, formal analysis. Taro Kato: writing - review and editing, conceptualization, formal analysis. Yoshihiro Horiuchi: conceptualization, formal analysis, writing - review and editing. Hiroshi Kirii: investigation, formal analysis, software, data curation. Hoang Duy Nguyen: investigation. Kenji Hinotsu: investigation, writing - review and editing. Yoshio Ohya: investigation. Takahiro Asada: investigation. Akiyoshi Yokode: investigation. Yuko Okahisa: supervision. Haruko Miyazaki: writing - review and editing, validation, methodology, supervision. Toshitaka Oohashi: methodology, supervision, funding acquisition, validation, writing - review and editing, resources, project administration. Manabu Takaki: conceptualization, methodology, validation, supervision, resources, project administration, writing - review and editing, funding acquisition.

Acknowledgments

The authors are grateful to the late Hidetoshi Morita for help with the gut microbiota analysis.

This work was supported by JSPS KAKENHI Grant Number 25K19080 (H.K.), 24K10679 (S.S.), 23H04235 (T.O.), 24K10733 (T.O.), 24KK0155 (T.O.), and 22K07616 (M.T.) as well as institutional grant of Okayama University, Oofuji Endocrine Medical Award 2023 (H.K.). This work was also supported by a collaborative research grant to Okayama University from Sumitomo Pharma Co. Ltd. (Japan). We would like to thank Editage (www.editage.jp) for English language editing.

Conflicts of Interest

Kenji Miyazaki, Taro Kato, and Yoshihiro Horiuchi were employees of Sumitomo Pharma Co. Ltd. at the time at which the study was conducted. There is no other conflicts of interest to report. However, the final interpretation of results and manuscript writing was independently conducted by the authors at Okayama University.

Data Availability Statement

The data that support the findings of this study are available from the corresponding author upon reasonable request.

References

Abuzeid, W., and C. Glover. 2011. "Acute Myocardial Infarction and Anorexia Nervosa." *International Journal of Eating Disorders* 44: 473–476.

Amorim, T., A. Khiyami, T. Latif, and P. K. Fazeli. 2023. "Neuroendocrine Adaptations to Starvation." *Psychoneuroendocrinology* 157: 106365.

Anagnostis, P., N. Katsiki, F. Adamidou, et al. 2013. "11beta-Hydroxysteroid Dehydrogenase Type 1 Inhibitors: Novel Agents for the Treatment of Metabolic Syndrome and Obesity-Related Disorders?" *Metabolism* 62: 21–33.

Andreani, N. A., A. Sharma, B. Dahmen, et al. 2024. "Longitudinal Analysis of the Gut Microbiome in Adolescent Patients With Anorexia Nervosa: Microbiome-Related Factors Associated With Clinical Outcome." *Gut Microbes* 16: 2304158.

Aston, S. A., B. S. Caffo, H. Bhasin, T. H. Moran, and K. L. Tamashiro. 2023. "Timing Matters: The Contribution of Running During Different Periods of the Light/Dark Cycle to Susceptibility to Activity-Based Anorexia in Rats." *Physiology & Behavior* 271: 114349.

Atkinson, H. C., and B. J. Waddell. 1997. "Circadian Variation in Basal Plasma Corticosterone and Adrenocorticotropin in the Rat: Sexual Dimorphism and Changes Across the Estrous Cycle." *Endocrinology* 138: 3842–3848.

Balsevich, G., A. Abizaid, A. Chen, I. N. Karatsoreos, and M. V. Schmidt. 2019. "Stress and Glucocorticoid Modulation of Feeding and Metabolism." *Neurobiology of Stress* 11: 100171.

Benjamini, Y., and Y. Hochberg. 1995. "Controlling the False Discovery Rate: A Practical and Powerful Approach to Multiple Testing." *Journal of the Royal Statistical Society. Series B, Statistical Methodology* 57: 289–300.

Berthiaume, M., M. Laplante, W. Festuccia, et al. 2007. "Depot-Specific Modulation of Rat Intraabdominal Adipose Tissue Lipid Metabolism by Pharmacological Inhibition of 11beta-Hydroxysteroid Dehydrogenase Type 1." *Endocrinology* 148: 2391–2397.

Bisschop, P. H., M. J. H. J. Dekker, W. Osterthun, et al. 2013. "Expression of 11β -Hydroxysteroid Dehydrogenase Type 1 in the Human Hypothalamus." *Journal of Neuroendocrinology* 25: 425–432.

Breton, J., P. Tirelle, S. Hasanat, et al. 2021. "Gut Microbiota Alteration in a Mouse Model of Anorexia Nervosa." *Clinical Nutrition* 40: 181–189.

Bridges, N., K. Slais, and E. Syková. 2008. "The Effects of Chronic Corticosterone on Hippocampal Astrocyte Numbers: A Comparison of Male and Female Wistar Rats." *Acta Neurobiologiae Experimentalis* 68: 131–138.

Chaaya, R., J. R. Steele, B. G. Oliver, H. Chen, and R. Machaalani. 2023. "Effects of e-Vapour and High-Fat Diet on the Immunohistochemical Staining of Nicotinic Acetylcholine Receptors, Apoptosis, Microglia and Astrocytes in the Adult Male Mouse Hippocampus." *Journal of Chemical Neuroanatomy* 132: 102303.

Chapman, K., M. Holmes, and J. Seckl. 2013. "11 β -Hydroxysteroid Dehydrogenases: Intracellular Gate-Keepers of Tissue Glucocorticoid Action." *Physiological Reviews* 93: 1139–1206.

Courtney, R., P. M. Stewart, M. Toh, M.-N. Ndongo, R. A. Calle, and B. Hirshberg. 2008. "Modulation of 11beta-Hydroxysteroid Dehydrogenase (11betaHSD) Activity Biomarkers and Pharmacokinetics of PF-00915275, a Selective 11betaHSD1 Inhibitor." *Journal of Clinical Endocrinology and Metabolism* 93: 550–556.

de Lartigue, G., and M. McDougle. 2019. "Dorsal Striatum Dopamine Oscillations: Setting the Pace of Food Anticipatory Activity." *Acta Physiologica* 225: e13152.

Di Lodovico, L., S. Mondot, J. Doré, I. Mack, M. Hanachi, and P. Gorwood. 2021. "Anorexia Nervosa and Gut Microbiota: A Systematic Review and Quantitative Synthesis of Pooled Microbiological Data." *Progress in Neuro-Psychopharmacology & Biological Psychiatry* 106: 110114.

Ding, J. X., P. T. Rudak, W. Inoue, and S. M. M. Haeryfar. 2021. "Physical Restraint Mouse Models to Assess Immune Responses Under Stress With or Without Habituation." *STAR Protocols* 2: 100838.

Dodd, S., D. R. Skvarc, O. M. Dean, A. Anderson, M. Kotowicz, and M. Berk. 2022. "Effect of Glucocorticoid and 11β -Hydroxysteroid-Dehydrogenase

- Type 1 (11β-HSD1) in Neurological and Psychiatric Disorders." *International Journal of Neuropsychopharmacology* 25: 387–398.
- Doerr, P., M. Fichter, K. M. Pirke, and R. Lund. 1980. "Relationship Between Weight Gain and Hypothalamic Pituitary Adrenal Function in Patients With Anorexia Nervosa." *Journal of Steroid Biochemistry* 13: 529–537.
- Droste, S. K., Y. Chandramohan, L. E. Hill, A. C. E. Linthorst, and J. M. H. M. Reul. 2007. "Voluntary Exercise Impacts on the Rat Hypothalamic-Pituitary-Adrenocortical Axis Mainly at the Adrenal Level." *Neuroendocrinology* 86: 26–37.
- Duclos, M., M. Bouchet, A. Vettier, and D. Richard. 2005. "Genetic Differences in Hypothalamic-Pituitary-Adrenal Axis Activity and Food Restriction-Induced Hyperactivity in Three Inbred Strains of Rats." *Journal of Neuroendocrinology* 17: 740–752.
- Duclos, M., C. Gatti, B. Bessière, and P. Mormède. 2009. "Tonic and Phasic Effects of Corticosterone on Food Restriction-Induced Hyperactivity in Rats." *Psychoneuroendocrinology* 34: 436–445.
- Fan, Y., R. K. Støving, S. Berreira Ibraim, et al. 2023. "The Gut Microbiota Contributes to the Pathogenesis of Anorexia Nervosa in Humans and Mice." *Nature Microbiology* 8: 787–802.
- Fediuc, S., J. E. Campbell, and M. C. Riddell. 2006. "Effect of Voluntary Wheel Running on Circadian Corticosterone Release and on HPA Axis Responsiveness to Restraint Stress in Sprague-Dawley Rats." *Journal of Applied Physiology* 100: 1867–1875.
- Fischer, S., R. Strawbridge, A. H. Vives, and A. J. Cleare. 2017. "Cortisol as a Predictor of Psychological Therapy Response in Depressive Disorders: Systematic Review and Meta-Analysis." *British Journal of Psychiatry* 210: 105–109.
- Frintrop, L., S. Trinh, J. Seitz, and M. Kipp. 2021. "The Role of Glial Cells in Regulating Feeding Behavior: Potential Relevance to Anorexia Nervosa." *Journal of Clinical Medicine* 11: 186.
- García-Rubira, J. C., R. Hidalgo, J. J. Gómez-Barrado, D. Romero, and J. M. Cruz Fernández. 1994. "Anorexia Nervosa and Myocardial Infarction." *International Journal of Cardiology* 45: 138–140.
- Gathercole, L. L., G. G. Lavery, S. A. Morgan, et al. 2013. " 11β -Hydroxysteroid Dehydrogenase 1: Translational and Therapeutic Aspects." *Endocrine Reviews* 34: 525–555.
- Glowa, J. R., J. E. Barrett, J. Russell, and P. W. Gold. 1992. "Effects of Corticotropin Releasing Hormone on Appetitive Behaviors." *Peptides* 13: 609–621.
- González-Vila, A., M. Luengo-Mateos, M. Silveira-Loureiro, et al. 2023. "Astrocytic Insulin Receptor Controls Circadian Behavior via Dopamine Signaling in a Sexually Dimorphic Manner." *Nature Communications* 14: 8175.
- Gupta, A., P. Chatelain, R. Massingham, E. N. Jonsson, and M. Hammarlund-Udenaes. 2006. "Brain Distribution of Cetirizine Enantiomers: Comparison of Three Different Tissue-to-Plasma Partition COEFFICIENTS: Kp, Kp,u, and Kp,uu." *Drug Metabolism and Disposition* 34: 318–323.
- Haines, M. S. 2023. "Endocrine Complications of Anorexia Nervosa." *Journal of Eating Disorders* 11: 24.
- Hermanowski-Vosatka, A., J. M. Balkovec, K. Cheng, et al. 2005. "11beta-HSD1 Inhibition Ameliorates Metabolic Syndrome and Prevents Progression of Atherosclerosis in Mice." *Journal of Experimental Medicine* 202: 517–527.
- Herpertz-Dahlmann, B., and H. Remschmidt. 1990. "The Prognostic Value of the Dexamethasone Suppression Test for the Course of Anorexia Nervosa—Comparison With Depressive Diseases." *Zeitschrift Für Kinder-Und Jugendpsychiatrie Und Psychotherapie* 18: 5–11.
- Het, S., S. Vocks, J. M. Wolf, S. Herpertz, and O. T. Wolf. 2020. "Treatment-Resistant Blunted HPA Activity, but Reversible Cardiovascular Stress

- Reactivity in Young Women With Eating Disorders." Frontiers in Psychiatry 11: 726.
- Horiuchi, Y., K. Sawamura, and H. Fujiwara. 2011. "WO-2011059021-A1–8-Azabicyclo[3.2.1]Octane-8-Carboxamide Derivative." https://portal.unifiedpatents.com/patents/patent/WO-2011059021-A1.
- Hu, G.-X., H. Lin, Q.-Q. Lian, et al. 2013. "Curcumin as a Potent and Selective Inhibitor of 11β -Hydroxysteroid Dehydrogenase 1: Improving Lipid Profiles in High-Fat-Diet-Treated Rats." *PLoS One* 8: e49976.
- Iwajomo, T., S. J. Bondy, C. de Oliveira, P. Colton, K. Trottier, and P. Kurdyak. 2021. "Excess Mortality Associated With Eating Disorders: Population-Based Cohort Study." *British Journal of Psychiatry* 219: 487–493.
- Jauregui-Huerta, F., Y. Ruvalcaba-Delgadillo, R. Gonzalez-Castañeda, J. Garcia-Estrada, O. Gonzalez-Perez, and S. Luquin. 2010. "Responses of Glial Cells to Stress and Glucocorticoids." *Current Immunology Reviews* 6: 195–204.
- Johnson, J. S., M. N. Opiyo, M. Thomson, et al. 2016. "11β-Hydroxysteroid Dehydrogenase-1 Deficiency Alters the Gut Microbiome Response to Western Diet." *Journal of Endocrinology* 232: 273–283.
- Joseph, D. N., and S. Whirledge. 2017. "Stress and the HPA Axis: Balancing Homeostasis and Fertility." *International Journal of Molecular Sciences* 18: 2224.
- Kawaguchi, M., K. A. Scott, T. H. Moran, and S. Bi. 2005. "Dorsomedial Hypothalamic Corticotropin-Releasing Factor Mediation of Exercise-Induced Anorexia." *American Journal of Physiology. Regulatory, Integrative and Comparative Physiology* 288: R1800–R1805.
- Kinzig, K. P., and S. L. Hargrave. 2010. "Adolescent Activity-Based Anorexia Increases Anxiety-Like Behavior in Adulthood." *Physiology & Behavior* 101: 269–276.
- Klindworth, A., E. Pruesse, T. Schweer, et al. 2013. "Evaluation of General 16S Ribosomal RNA Gene PCR Primers for Classical and Next-Generation Sequencing-Based Diversity Studies." *Nucleic Acids Research* 41: e1.
- Kooij, K. L., N. A. Andreani, L. Keller, et al. 2025. "Antibiotic-Induced Microbial Dysbiosis Worsened Outcomes in the Activity-Based Anorexia Model." *International Journal of Eating Disorders* 58: 1487–1498.
- Krahn, D. D., B. A. Gosnell, A. S. Levine, and J. E. Morley. 1988. "Behavioral Effects of Corticotropin-Releasing Factor: Localization and Characterization of Central Effects." *Brain Research* 443: 63–69.
- Lawson, E. A., L. M. Holsen, R. Desanti, et al. 2013. "Increased Hypothalamic-Pituitary-Adrenal Drive Is Associated With Decreased Appetite and Hypoactivation of Food Motivation Neurocircuitry in Anorexia Nervosa." European Journal of Endocrinology / European Federation of Endocrine Societies 169: 639–647.
- Layé, S., S. Liège, K. S. Li, E. Moze, and P. J. Neveu. 2001. "Physiological Significance of the Interleukin 1 Receptor Accessory Protein." *Neuroimmunomodulation* 9: 225–230.
- Lee, T.-J., and K. P. Kinzig. 2017. "Reprint of "Repeated Adolescent Activity-Based Anorexia Influences Central Estrogen Signaling and Adulthood Anxiety-Like Behaviors in Rats"." *Physiology & Behavior* 178: 179–186.
- Loerz, C., C. Staab-Weijnitz, P. Huebbe, et al. 2017. "Regulation of 11β-Hydroxysteroid Dehydrogenase Type 1 Following Caloric Restriction and Re-Feeding Is Species Dependent." *Chemico-Biological Interactions* 276: 95–104.
- Luijerink, L., M. Rodriguez, and R. Machaalani. 2024. "Quantifying GFAP Immunohistochemistry in the Brain Introduction of the Reactivity Score (R-Score) and How It Compares to Other Methodologies." *Journal of Neuroscience Methods* 402: 110025.
- Markopoulou, K., S. Fischer, A. Papadopoulos, et al. 2021. "Comparison of Hypothalamo-Pituitary-Adrenal Function in Treatment Resistant Unipolar and Bipolar Depression." *Translational Psychiatry* 11: 1–8.

- Menzaghi, F., R. L. Howard, S. C. Heinrichs, W. Vale, J. Rivier, and G. F. Koob. 1994. "Characterization of a Novel and Potent Corticotropin-Releasing Factor Antagonist in Rats." *Journal of Pharmacology and Experimental Therapeutics* 269: 564–572.
- Mogami, S., C. Sadakane, M. Nahata, et al. 2016. "CRF Receptor 1 Antagonism and Brain Distribution of Active Components Contribute to the Ameliorative Effect of Rikkunshito on Stress-Induced Anorexia." *Scientific Reports* 6: 27516.
- Mohawk, J. A., J. M. Pargament, and T. M. Lee. 2007. "Circadian Dependence of Corticosterone Release to Light Exposure in the Rat." *Physiology & Behavior* 92: 800–806.
- Moisan, M. P., J. R. Seckl, and C. R. Edwards. 1990. "11 Beta-Hydroxysteroid Dehydrogenase Bioactivity and Messenger RNA Expression in Rat Forebrain: Localization in Hypothalamus, Hippocampus, and Cortex." *Endocrinology* 127: 1450–1455.
- Mottarlini, F., G. Targa, B. Rizzi, F. Fumagalli, and L. Caffino. 2024. "Developmental Activity-Based Anorexia Alters Hippocampal Non-Genomic Stress Response and Induces Structural Instability and Spatial Memory Impairment in Female Rats." *Progress in Neuro-Psychopharmacology & Biological Psychiatry* 134: 111065.
- Namvar, S., A. Gyte, M. Denn, B. Leighton, and H. D. Piggins. 2016. "Dietary Fat and Corticosterone Levels Are Contributing Factors to Meal Anticipation." *American Journal of Physiology. Regulatory, Integrative and Comparative Physiology* 310: R711–R723.
- Nguyen, H. D., H. Miyazaki, H. Kawai, et al. 2025. "Alteration of Perineuronal Nets and Parvalbumin Interneurons in Prefrontal Cortex and Hippocampus, and Correlation With Blood Corticosterone in Activity-Based Anorexia Model Mice." *Neuroscience Research* 218: 104922.
- Othonos, N., R. Pofi, A. Arvaniti, et al. 2023. "11 β -HSD1 Inhibition in Men Mitigates Prednisolone-Induced Adverse Effects in a Proof-Of-Concept Randomised Double-Blind Placebo-Controlled Trial." *Nature Communications* 14: 1025.
- Park, J. S., S. J. Bae, S.-W. Choi, et al. 2014. "A Novel 11β -HSD1 Inhibitor Improves Diabesity and Osteoblast Differentiation." *Journal of Molecular Endocrinology* 52: 191–202.
- Patton, D. F., and R. E. Mistlberger. 2013. "Circadian Adaptations to Meal Timing: Neuroendocrine Mechanisms." *Frontiers in Neuroscience* 7: 185
- Podraza, J., K. Gutowska, A. Lenartowicz, et al. 2024. "The Role of microRNA in the Regulation of Cortisol Metabolism in the Adipose Tissue in the Course of Obesity." *International Journal of Molecular Sciences* 25: 5058.
- Ragu-Varman, D., M. Macedo-Mendoza, F. E. Labrada-Moncada, et al. 2019. "Anorexia Increases Microglial Density and Cytokine Expression in the Hippocampus of Young Female Rats." *Behavioural Brain Research* 363: 118–125.
- Rajan, V., C. R. Edwards, and J. R. Seckl. 1996. "11 Beta-Hydroxysteroid Dehydrogenase in Cultured Hippocampal Cells Reactivates Inert 11-Dehydrocorticosterone, Potentiating Neurotoxicity." *Journal of Neuroscience* 16: 65–70.
- Reyes-Haro, D., F. E. Labrada-Moncada, D. R. Varman, et al. 2016. "Anorexia Reduces GFAP+ Cell Density in the Rat Hippocampus." *Neural Plasticity* 2016: 2426413.
- Saavedra, L. M., B. Fenton Navarro, and L. Torner. 2018. "Early Life Stress Activates Glial Cells in the Hippocampus but Attenuates Cytokine Secretion in Response to an Immune Challenge in Rat Pups." *Neuroimmunomodulation* 24: 242–255.
- Sandeep, T. C., J. L. W. Yau, A. M. J. MacLullich, et al. 2004. "11β-Hydroxysteroid Dehydrogenase Inhibition Improves Cognitive Function in Healthy Elderly Men and Type 2 Diabetics." *Proceedings of the National Academy of Sciences of the United States of America* 101: 6734–6739.

- Schalla, M. A., and A. Stengel. 2019. "Activity Based Anorexia as an Animal Model for Anorexia Nervosa–A Systematic Review." *Frontiers in Nutrition* 6: 69.
- Schmalbach, I., B. Herhaus, S. Pässler, et al. 2020. "Cortisol Reactivity in Patients With Anorexia Nervosa After Stress Induction." *Translational Psychiatry* 10: 1–15.
- Schulz, N., M. Belheouane, B. Dahmen, et al. 2021. "Gut Microbiota Alteration in Adolescent Anorexia Nervosa Does Not Normalize With Short-Term Weight Restoration." *International Journal of Eating Disorders* 54: 969–980.
- Schweitzer, I., G. I. Szmukler, K. P. Maguire, L. C. Harrison, V. Tuckwell, and B. M. Davies. 1990. "The Dexamethasone Suppression Test in Anorexia Nervosa. The Influence of Weight, Depression, Adrenocorticotrophic Hormone and Dexamethasone." *British Journal of Psychiatry* 157: 713–717.
- Sheward, W. J., E. S. Maywood, K. L. French, et al. 2007. "Entrainment to Feeding but Not to Light: Circadian Phenotype of VPAC2 Receptor-Null Mice." *Journal of Neuroscience* 27: 4351–4358.
- Silver, R., and P. Balsam. 2010. "Oscillators Entrained by Food and the Emergence of Anticipatory Timing Behaviors." *Sleep Biology Rhythms* 8: 120–136.
- Spina, M. G., A. M. Basso, E. P. Zorrilla, et al. 2000. "Behavioral Effects of Central Administration of the Novel CRF Antagonist Astressin in Rats." *Neuropsychopharmacology* 22: 230–239.
- Stomby, A., R. Andrew, B. R. Walker, and T. Olsson. 2014. "Tissue-Specific Dysregulation of Cortisol Regeneration by 11β HSD1 in Obesity: Has It Promised Too Much?" *Diabetologia* 57: 1100–1110.
- Treasure, J., T. A. Duarte, and U. Schmidt. 2020. "Eating Disorders." *Lancet* 395: 899–911.
- Trinh, S., V. Kogel, C. Voelz, et al. 2021. "Gut Microbiota and Brain Alterations in a Translational Anorexia Nervosa Rat Model." *Journal of Psychiatric Research* 133: 156–165.
- van de Wouw, M., H. Schellekens, T. G. Dinan, and J. F. Cryan. 2017. "Microbiota-Gut-Brain Axis: Modulator of Host Metabolism and Appetite." *Journal of Nutrition* 147: 727–745.
- van Eeden, A. E., D. van Hoeken, and H. W. Hoek. 2021. "Incidence, Prevalence and Mortality of Anorexia Nervosa and Bulimia Nervosa." *Current Opinion in Psychiatry* 34: 515–524.
- Watson, H. J., Z. Yilmaz, L. M. Thornton, et al. 2019. "Genome-Wide Association Study Identifies Eight Risk Loci and Implicates Metabo-Psychiatric Origins for Anorexia Nervosa." *Nature Genetics* 51: 1207–1214.
- Wiklund, C. A., M. Rania, R. Kuja-Halkola, L. M. Thornton, and C. M. Bulik. 2021. "Evaluating Disorders of Gut-Brain Interaction in Eating Disorders." *International Journal of Eating Disorders* 54: 925–935.
- Windle, R. J., S. A. Wood, N. Shanks, S. L. Lightman, and C. D. Ingram. 1998. "Ultradian Rhythm of Basal Corticosterone Release in the Female Rat: Dynamic Interaction With the Response to Acute Stress*." *Endocrinology* 139: 443–450.
- Yau, J. L. W., J. Noble, C. J. Kenyon, M. Ludwig, and J. R. Seckl. 2015. "Diurnal and Stress-Induced Intra-Hippocampal Corticosterone Rise Attenuated in 11β -HSD1-Deficient Mice: A Microdialysis Study in Young and Aged Mice." *European Journal of Neuroscience* 41: 787–792.
- Yau, J. L. W., N. Wheelan, J. Noble, et al. 2015. "Intrahippocampal Glucocorticoids Generated by 11 β -HSD1 Affect Memory in Aged Mice." *Neurobiology of Aging* 36: 334–343.
- Yoshimura, M., B. P. Flynn, Y. M. Kershaw, et al. 2023. "Phase-Shifting the Circadian Glucocorticoid Profile Induces Disordered Feeding Behaviour by Dysregulating Hypothalamic Neuropeptide Gene Expression." *Communications Biology* 6: 1–13.

Yuan, R., L. Yang, G. Yao, et al. 2022. "Features of Gut Microbiota in Patients With Anorexia Nervosa." *Chinese Medical Journal* 135: 1993–2002.

Zhang, H., Y. Zhao, and Z. Wang. 2015. "Chronic Corticosterone Exposure Reduces Hippocampal Astrocyte Structural Plasticity and Induces Hippocampal Atrophy in Mice." *Neuroscience Letters* 592: 76–81.

Zhang, J., and S. C. Dulawa. 2021. "The Utility of Animal Models for Studying the Metabo-Psychiatric Origins of Anorexia Nervosa." *Frontiers in Psychiatry* 12: 711181.

Zhang, M., Z. Shi, C. Wu, et al. 2024. "Cushing Syndrome Is Associated With Gut Microbial Dysbiosis and Cortisol-Degrading Bacteria." *Journal of Clinical Endocrinology and Metabolism* 109: 1474–1484.

Zhang, Q., G. Guan, J. Liu, W. Hu, and P. Jin. 2024. "Gut Microbiota Dysbiosis and Decreased Levels of Acetic and Propionic Acid Participate in Glucocorticoid-Induced Glycolipid Metabolism Disorder." *MBio* 15: e0294323.

Zimmermann, A., N. Böge, K. Schuster, et al. 2023. "Glial Cell Changes in the Corpus Callosum in Chronically-Starved Mice." *Journal of Eating Disorders* 11: 227.

Zimmermann, A., J. Priebe, H. Rupprecht, et al. 2025. "Changes in Circadian Rhythm in Chronically-Starved Mice Are Associated With Glial Cell Density Reduction in the Suprachiasmatic Nucleus." *International Journal of Eating Disorders* 58, no. 4: 756–769.

Zipfel, S., I. Mack, L. A. Baur, et al. 2013. "Impact of Exercise on Energy Metabolism in Anorexia Nervosa." *Journal of Eating Disorders* 1: 37.